C. R. Physique 11 (2010) 433–443

Contents lists available at ScienceDirect

Comptes Rendus Physique

www.sciencedirect.com

Terahertz electronic and optoelectronic components and systems

Plasma excitations in field effect transistors for terahertz detection and emission

Excitation d'ondes plasma dans les transistors à effet de champ pour la génération et la détection d'ondes térahertz

W. Knap [a,*], D. Coquillat [a], N. Dyakonova [a], F. Teppe [a], O. Klimenko [a], H. Videlier [a], S. Nadar [a], J. Łusakowski [b], G. Valusis [c], F. Schuster [a,d], B. Giffard [d], T. Skotnicki [e], C. Gaquière [f], A. El Fatimy [g]

[a] *GES UMR 5650, Université Montpellier 2 and CNRS, Place E. Bataillon, 34950 Montpellier, France*
[b] *Institute of Experimental Physics, University of Warsaw, ul. Hoża 69, 00-681 Warsaw, Poland*
[c] *Center for Physical Sciences and Technology, Savanoriu ave. 231, 02300, Vilnius, Lithuania*
[d] *CEA-LETI, MINATEC, CEA-Grenoble, 17, rue des Martyrs, 38054 Grenoble cedex 9, France*
[e] *ST Microelectronics, BP 16, 38921 Crolles, France*
[f] *IEMN, UMR CNRS 8520, 59655 Villeneuve d'Ascq, France*
[g] *School of Physics and Astronomy, Cardiff University, Cardiff CF24 3AA, United Kingdom*

ARTICLE INFO

Article history:
Available online 24 July 2010

Keywords:
Field effect transistor
Terahertz

Mots-clés :
Transistor à effet de champ
Térahertz

ABSTRACT

Resonant frequencies of the two-dimensional plasma in field effect transistors (FETs) increase with the reduction of the channel dimensions and can reach the THz range for nanometer size devices. Nonlinear properties of the electron plasma in the transistor channel can lead to the detection and emission of THz radiation. The excitation of plasma waves by sub-THz and THz radiation was experimentally demonstrated at cryogenic as well as at room temperatures. We present an overview of experimental results on THz detection by FETs discussing possibilities of improvement of their performance and application for THz room temperature imaging. We present also recent results on THz emission from GaN/AlGaN-based FETs.

RÉSUMÉ

Les fréquences de résonance de plasma bidimensionnel dans les transistors à effet de champ (FET) augmentent quand la taille du canal du transistor diminue, et ainsi peuvent atteindre le domaine térahertz pour des canaux nanométriques. Les propriétés non linéaires du plasma électronique dans le canal du FET permettent la génération et la détection du rayonnement THz. L'excitation de ces ondes plasma par un rayonnement sub-THz et THz a été démontrée expérimentalement à des températures cryogéniques mais aussi ambiantes. Nous présentons une revue des résultats expérimentaux de détection des ondes THz à l'aide de FET et nous discutons des possibilités d'amélioration de leurs

* Corresponding author.
E-mail address: knap@ges.univ-montp2.fr (W. Knap).

1631-0705/$ – see front matter
doi:10.1016/j.crhy.2010.06.010

performances en vue d'application pour l'imagerie THz à température ambiante. Nous présentons aussi des résultats récents de l'émission THz par des FET à base de GaN/AlGaN.

1. Introduction

The channel of a field effect transistor (FET) can act as a resonator for plasma waves. The frequency of plasma waves propagating in this resonator depends on its dimensions, and can reach the sub-Terahertz or Terahertz (THz) range for gate lengths of micron and submicron (nanometer) size. The interest in the applications of FETs for THz spectroscopy started at early 1990s with a pioneering theoretical work of Dyakonov and Shur [1] who predicted that a steady current flow in a FET channel can become unstable against generation of plasma waves. These waves can, in turn, lead to the emission of electromagnetic radiation at the plasma wave frequency. This work was followed by another, where the same authors have shown that nonlinear properties of the 2D plasma in the transistor channel can be used for detection of THz radiation [2]. THz emission in nW power range from submicron InGaAs and GaN FETs has been observed both at cryogenic and room temperatures [3–5]. THz detection by FETs is due to nonlinear properties of the transistor, which lead to the rectification of the ac current induced by the incoming radiation. As a result, a photoresponse appears in the form of a dc voltage between source and drain. This voltage is proportional to the radiation intensity (photovoltaic effect). More information on the state-of-the-art of the FETs as THz emitters and detectors can be found in review papers [6–8].

In the present article, we present an overview of most recent results concerning THz detection and emission by FETs. The article is organized as follows. Section 1 is the introduction summarizing some first most important experimental results in a chronological order. Section 2 describes recent results on room temperature imaging at 1.6 THz and 2.5 THz [9]. Section 3 concerns the influence of magnetic field on THz detection by FETs [10–12]. In Section 4 THz detection and imaging by silicon-based FETs is presented [13,14]. Finally, Section 5 summarizes the experimental results on THz emission from FETs, and describes recent results on gate tunable THz emission from GaN based transistors [15].

The layout of a typical commercial device used in many experiments is shown in Fig. 1. Usually, in detection experiments, the transistors are illuminated with a monochromatic beam generated either by an electronic source (e.g., a Gunn diode), a backward wave oscillator (BWO), or a CO_2-pumped molecular THz laser. In the absence of an antenna, the THz radiation is coupled to the FET by contact pads and bonding wires, so the amount of THz radiation that is coupled to the device is not very high. Hence, a big progress in sensitivity can be obtained by adding a proper antenna or a cavity coupling.

As can be seen in Fig. 1, the geometry of metalization is such that the capacitance between the source and the gate is bigger than that between the drain and the gate contacts. This asymmetry defines the sign of the signal for a uniform illumination of the device. The experiments with a polarized radiation show usually a well defined preferential orientation of the electric field of the incident radiation. This orientation is defined by the geometry of metalization of the contacts (playing the role of an antenna) or by the bonding wires [16]. The black solid line in Fig. 1 shows the amplitude of the photoresponse versus the polarization angle obtained with a linearly polarized radiation. The maximum in the signal is observed when the polarization of the incoming radiation is such that the maximal ac voltage is created between the drain and gate contacts. The mechanism of radiation coupling was also studied in [17].

Typical results of detection experiments are shown in Fig. 2 [18]. A photovoltaic signal between source and drain is recorded versus the gate voltage, i.e. versus the carrier density in the channel. In Fig. 2(a), the recorded signal is presented for two transistors with different threshold voltages. For a high carrier density (open channel), the signal is relatively small and increases when the gate voltage approaches the threshold. This increase follows a $1/(V_g - V_{th})$ functional dependence. However, the signal does not diverge when V_g approaches V_{th} but it usually shows a broad maximum. As can be seen

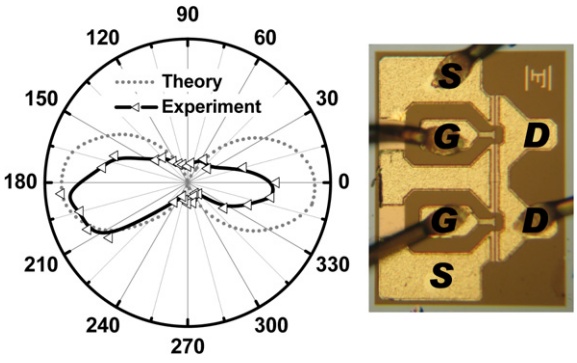

Fig. 1. The amplitude of the photovoltaic signal versus polarization angle (left) and the layout of a typical commercial FET device used in the experiments (right). The solid line in the graph corresponds to experimental results and dotted line is a theoretical fit for the preferential polarization direction along the gate–drain direction [16].

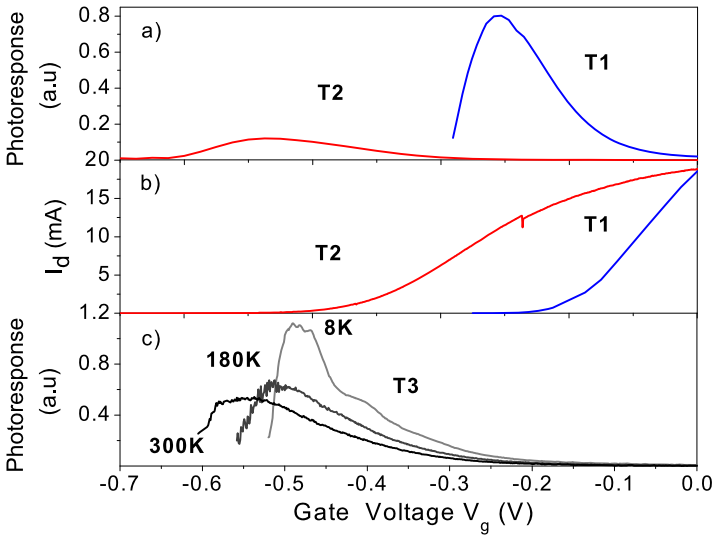

Fig. 2. (a) Experimental photoresponse for two GaAs/AlGaAs transistors T1 and T2. Curves marked T1 correspond to a transistor with the threshold voltage $V_{th} = -0.55$ V; detection signal was measured at 300 K and 200 GHz. Curves marked T2 correspond to another transistor with the threshold voltage $V_{th} = -0.22$ V; detection signal was measured at 210 K and 100 GHz. (b) Transfer characteristics (the drain current versus the gate voltage V_g at a constant source–drain voltage) for T1 and T2 transistors. (c) Photoresponse of a transistor T3 with the gate length $L = 0.15$ μm as a function of the gate voltage at 600 GHz. Note a shift of the threshold voltage with temperature. The result at 8 K shows a signature of a resonant structure.

by comparing the photovoltaic signal (Fig. 2(a)) and the transfer characteristics (Fig. 2(b)), the position of the maximum correlates with the threshold voltage. The shape and the position of the maximum depend also on loading effects [19,18]: close to the threshold, the channel resistance tends to infinity and the transistor behaves like a voltage source with a very high internal resistance. The signal limitation close to the threshold voltage can be also due to gate leakage currents [18]. The detection curves like these shown in Fig. 2(a) are related to a broadband nonresonant detection. The position and the shape of the maximum depends also strongly on temperature because the carrier density (or the threshold voltage), the channel resistance and the gate leakage current depend strongly on temperature. This is illustrated in Fig. 2(c) where results for the same transistor at three different temperatures are shown. The maximum of detection shifts to the lower gate voltage with decrease of temperature. For the lowest temperature one can observe an additional maximum appearing on the $1/(V_g - V_{th})$ like shoulder. This maximum is a signature of the resonant detection.

Examples of a resonant detection are shown in Figs. 3 and 4 [20,21]. We show experimental traces as well as the theoretical fits in the region above the threshold where artifacts related to the measurement system (resistive and capacitive coupling and gate leakage problems) can be neglected. As already mentioned above, in a majority of experiments, the incoming radiation is a monochromatic beam and the source–drain voltage is recorded versus the gate voltage. The gate voltage controls the carrier density in the channel and therefore allows the resonant plasma frequency to be tuned. A resonant enhancement of the registered voltage is observed once the resonant plasma frequency coincides with the frequency of the incoming THz radiation. The resonance appears at low temperatures because the carrier mobility increases and $\omega\tau > 1$ condition can be reached ($\omega = 2\pi f$ is the excitation frequency and τ is the electron momentum relaxation time). Fig. 3(b) shows the results of the fits according the theory [2]. One can see that both the slope of the detected signal as well as appearance of the resonance can be well reproduced [20,21].

First detection experiments showing a resonant structure in the signal were performed using submicron GaAs/AlGaAs HEMTs [20,21]. Subsequently, high mobility InGaAs/InAlAs transistors were studied [22]. Fig. 4(a) shows an example of a plasma related resonant detection for these transistors at 1.8 THz, 2.5 THz and 3.1 THz.

In Fig. 4(b), the position of the resonant maximum is shown. As the excitation frequency increases from 1.8 THz to 3.1 THz, the plasma resonance moves to higher swing voltages in an approximate agreement with theoretical predictions (solid line). However, the resonance is much broader than theoretically expected.

An important plasma resonance broadening appears to be one of the main unresolved problems of the resonant THz detection by FETs. A convenient way to discuss the broadening is to consider the quality factor $Q = \omega\tau$. From the experimental point of view, Q describes the ratio of the resonant line position (in frequency or voltage) with respect to the line width.

For $Q \gg 1$ one expects pronounced narrow peaks of plasma resonances. For $Q \ll 1$, the plasma oscillations are overdamped; consequently, the response is expected to show a nonresonant, monotonic behavior. The main motivation behind changing the transistor material system from GaAs/GaAlAs, as used in first experiments [20,21], to InGaAs/InP [22] and using higher excitation frequencies (up to 3 THz instead of 0.6 THz) was to improve the quality factor.

A longer carrier scattering time (higher mobility) combined with the use of higher excitation frequencies was expected to result in an increase of the quality factor by at least an order of magnitude, leading to sharp plasma resonances. However,

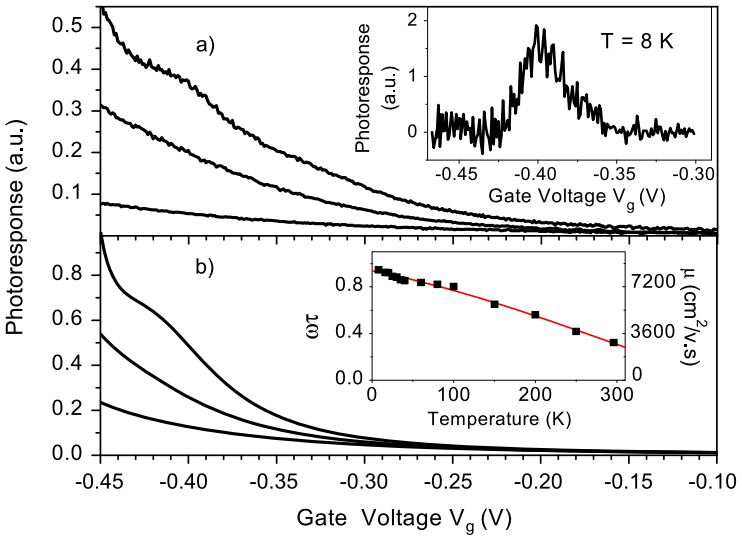

Fig. 3. The photoresponse versus gate voltage in the region above the threshold: (a) experiment and (b) theory. The evolution of the photoresponse with decrease of the temperature (300 K, 180 K to 8 K, bottom to top) and appearance of the resonant structure are illustrated. Insert in (a) shows the resonant signal after subtraction of the background. Insert in (b) shows the evolution of the carrier mobility and the corresponding quality factor at 600 GHz radiation (after Refs. [7,20,21]).

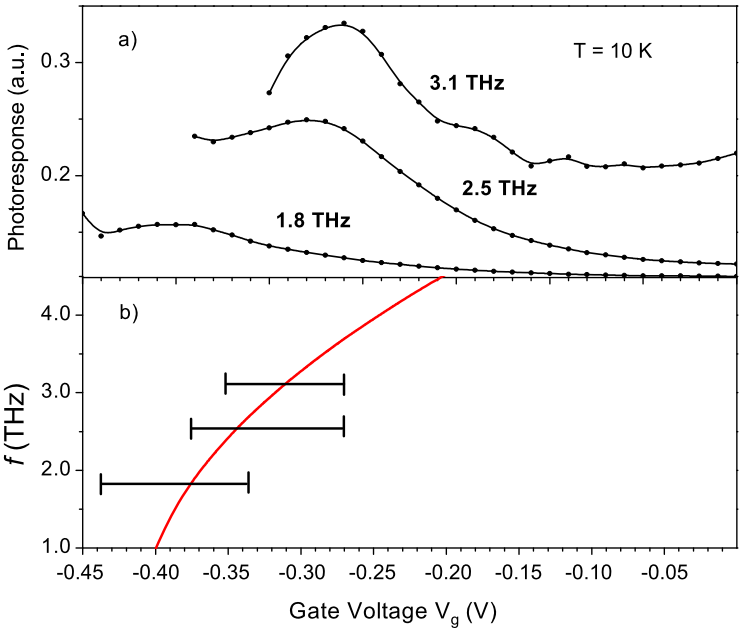

Fig. 4. (a) A resonant response of high mobility InGaAs/InAlAs transistors at 1.8 THz, 2.5 THz and 3.1 THz registered at 10 K. (b) Position of the signal maximum versus the gate voltage. Solid line is a result of calculation [22].

the experimentally observed plasma resonances remained broad. Even at 3 THz the quality factor Q was never higher than 2–3. Understanding the origin of the broadening and minimizing it is one of the most important experimental and theoretical challenges up to now.

Two main hypotheses on the origin of an additional broadening are currently under consideration: (i) the existence of oblique plasma modes [23] and (ii) an additional damping due to the leakage of gated plasmons to ungated parts of the transistor channel [24]. The first hypothesis is related to the fact that in realistic devices the gate width is much greater than the gate length. In such a case, plasma waves can propagate not only in the source–drain direction but also in oblique directions. The spectrum of plasma waves in this case is continuous, with a cut-off at low frequency. The second hypothesis, a leakage of gated plasmons to ungated parts of the channel [24], is related to the fact that in HEMTs investigated the gate covers only a small part of the source–drain distance. Therefore, the plasma under the gate can not be treated independently

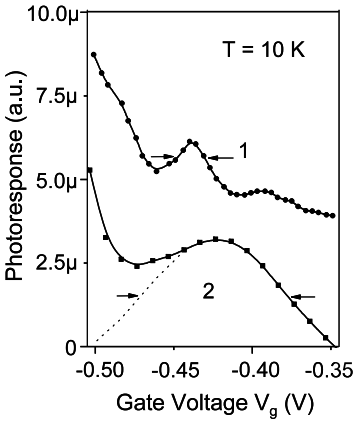

Fig. 5. Photoresponse at 10 K as a function of the gate voltage. Curve 2 was obtained at 2.5 THz with a conventional InGaAs HEMT. Curve 1 was obtained at 540 GHz with a multi-channel InGaAs HEMT at zero drain—to source voltage. Curves are vertically shifted.

of the plasma in ungated parts. An interaction between the two plasma regions can lead not only to a modification of the resonant frequency [25,26], but also to a mode leakage followed by a shortening of the gated plasmon lifetimes and hence the line broadening.

To decrease the role of oblique modes, one has to change the geometry of the channel. One can, for example, replace a wide single channel by a series of many narrow channels [27,28]. In Fig. 5 we present a comparison of the photoresponse at 2.5 THz of a conventional InGaAs HEMT (curve 2, squares), with that of a narrow multichannel transistor at 540 GHz (curve 1, circles). One can clearly see the narrowing of the resonant line.

In experiments with a multi-channel InGaAs HEMT, the channel length was only 2 times larger than the width. Therefore, the plasmon spectrum showed a complicated multimode structure. This result clearly shows, however, that use of FETs with narrow (one-dimensional) channels is the best way to get a high quality factor the plasmon resonance.

Another important point that should be considered is the way how a nanotransistor couples to THz radiation. As already mentioned above, most experiments were performed on FETs without any special antennas. In the absence of an antenna the THz radiation is coupled to the FET by contact pads and bonding wires. The amount of THz radiation that is coupled to the device is rather small, and a big progress in sensitivity can be obtained by adding a proper antenna or a cavity coupling. One of the efficient way of coupling is the use the gratings. The study of the grating coupling was recently presented in Refs. [29] and [30].

2. 1.6 THz and 2.5 THz room temperature imaging with FETs

At room temperature, FET can operate as an efficient broadband detector of sub-THz radiation. Recently, Lisauskas et al. have reported the possibility of sub-THz (0.6 THz) imaging with GaAs/AlGaAs FET [31,32]. However, up to now, there are only a very few results on imaging with FETs at frequencies above 1 THz. In a broadband nonresonant detection regime, the photovoltaic signal decreases strongly with the increase of the radiation frequency either because of a reduced coupling efficiency or an efficiency of rectification mechanism itself due to parasitic capacitances. El Fatimy et al. [33] have reported images obtained in a transmission mode by using a coherent broadband THz pulsed radiation source and a GaAs/AlGaAs FET driven by 40 mA drain to source current.

In Fig. 6, we present 2D images obtained with a CO_2 pumped far infrared laser radiation of 1.6 THz and a GaAs/AlGaAs FET HEMT operating at room temperature [34]. A particular feature of this work consist in (i) imaging at a frequency above 1 THz to improve the spatial resolution and (ii) studying the effect of applied drain current on the contrast of the image. The images in Fig. 6 were recorded in a transmission mode by raster scanning the sample in X and Y directions. These results show that room temperature GaAs/AlGaAs FETs can be efficiently used at 1.6 THz for imaging systems, with a short time integration (50 ms) and a useful resolution (300 μm).

First results at 2.5 THz were also obtained (Fig. 6(b)). The signal/noise ratio was not sufficient to demonstrate an improvement of the spatial resolution. However, the image shows that room temperature imaging using GaAs/AlGaAs FETs at frequencies up to 2.5 THz is possible upon condition of improvement of the responsivity. This can be achieved by a better antenna coupling or application of the drain current [34].

3. Detection in quantizing magnetic fields

Very interesting physical effects were recently observed while studying THz detection in quantizing magnetic fields. The photovoltaic detection signal was investigated as a function of the gate voltage and magnetic field using InGaAs/InAlAs FETs and GaAs/AlGaAs FETs. Oscillations analogous to the Shubnikov–de Haas oscillations as well as their strong modification at the cyclotron resonance condition were observed [10,12]. The results allowed to reveal the influence gated

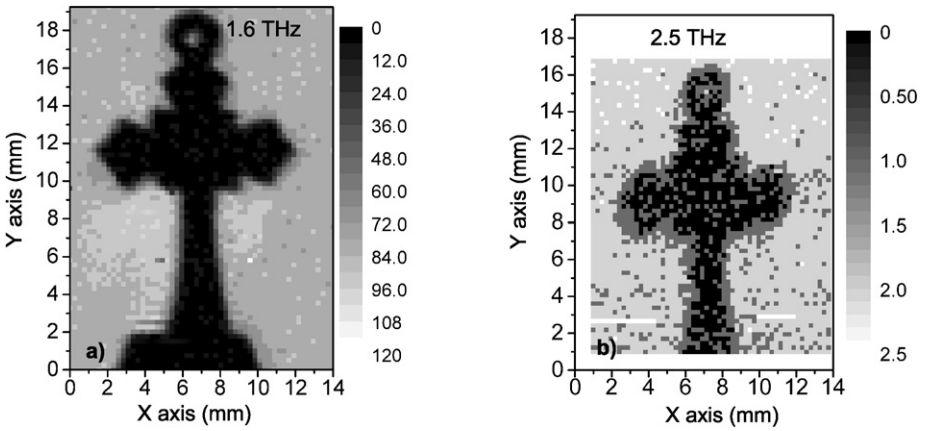

Fig. 6. THz images of a metallic cross in the transmission mode at room temperature at 1.6 THz and 2.5 THz.

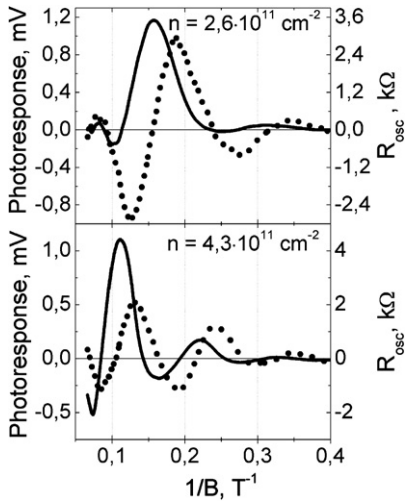

Fig. 7. The photovoltaic response at 1.0 THz (solid curves) and the oscillating part of the magnetoresistance R_{osc} (dotted curves) of InGaAs HEMT versus inversed magnetic field, measured at different electron concentrations in the transistor channel.

and ungated parts of the channel to the detection signal [11] and were interpreted within a recently developed theory [35].

In the theoretical work, two major effects are predicted. The first one is an oscillating Shubnikov–de Haas-like component of the detection signal with a singularity in the vicinity of the cyclotron resonance. The second effect is the presence of a component unrelated to Shubnikov–de Haas oscillations. A strong modification of the signal close to cyclotron resonance is related to the fact that in the gated region of the channel plasma waves can propagate only if the cyclotron resonance frequency is lower than the radiation frequency. In the opposite case, the plasma wave vector becomes imaginary and plasma oscillations are damped.

Experimental studies were carried out at liquid helium temperatures at 1.0 THz and 2.5 THz incident radiation.

In Fig. 7 we show the results of simultaneous measurements of magnetoresistance (dot line) and the photovoltaic effect (solid line) for the radiation frequency of 1.0 THz.

The measured photoresponse dependences as functions of magnetic field, B, revealed a pronounced oscillating behavior periodic with $1/B$. The amplitude of the photoresponse signal but also its polarity oscillated with the magnetic field. The measured magnetoresistance also revealed oscillations periodic in $1/B$, correlated with those of the photoresponse (Fig. 7). The period of both types of oscillations was the same and depended on the gate voltage in the same manner. A strong correlation of the two effects may be considered as a direct experimental confirmation that the observed photoresponse is related to the electron plasma in the gated part of the transistor channel. The most remarkable effect is a $\pi/2$ phase shift between the photoresponse and magnetoresistance oscillations. Both effects (the periodicity and the phase shift) are predicted by Lifshits–Dyakonov theory [35].

In Fig. 8 experiments at 2.5 THz are compared with calculations based on the model of Ref. [35]. Fig. 8 (top panels) shows FET signal as a function of the magnetic field for two different electron densities. The experiments show not only an oscillatory character of the signal and its periodicity versus $1/B$, but also a strong modification of the signal in the

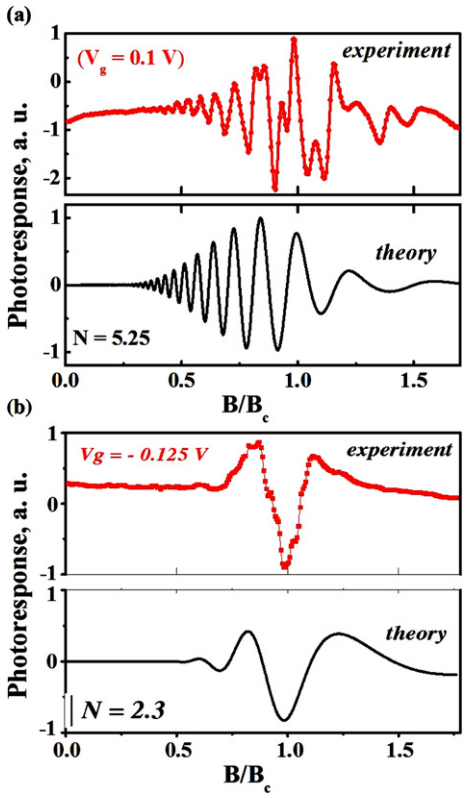

Fig. 8. (a) Top: experimental photoresponse as a function of the magnetic field for $V_g = 0.1$ V—high carrier density. Bottom: calculations using Eq. (1) of Ref. [35]. (b) Same as in (a) for lower electron density ($V_g = -0.125$ V).

vicinity of the cyclotron resonance. Shubnikov–de Haas-like photovoltaic signal is damped for magnetic fields higher than that corresponding to the cyclotron resonance. This damping was not observed at 1 THz experiment because the cyclotron resonance appeared in much smaller magnetic fields. Lower panels in Fig. 8 show calculations of the FET signal, using the oscillating part of Eq. (1) in Ref. [35]. The theory describes correctly an influence of Shubnikov–de Haas effect on the photoresponse as well as the plasma wave damping in the post-cyclotron resonance region. This damping is reflected in a reduction of the induced signal, as can be seen in Fig. 8.

The reduction of the photo-induced signal above the cyclotron resonance and its change with the gate voltage confirm once more that indeed plasma waves excited in the gated part of the transistor are involved in the detection. One can see also that at a low carrier density an enhancement of the signal at the cyclotron resonance condition can be obtained. This phenomenon can lead to a new class of THz detectors—selective and magnetic field-tunable plasma wave detectors. We would like to stress here that to get an agreement with experimental data we had to neglect the nonresonant part of the formula of Ref. [35]. This result indicates that further theoretical research is necessary to fully explain the experiments.

4. Detection by Si-MOSFETs

FETs fabricated in Si-CMOS technology have been shown to be very promising for room temperature THz detection [31,32] and were successfully used for imaging at frequency below 1 THz [33,34]. To determine the best FET parameters for THz detection, Si FETs were studied as a function of their gate length.

Fully depleted nMOS transistors were fabricated on a biaxially strained SOI. The gate length, L_g, was in the range from 50 nm to 10 μm. The channel depletion threshold voltage was near 0.2 V. Photoresponse measurements were performed at room temperature using a BWO operating at 0.23 THz. Fig. 9 shows a photoresponse of FETs with different gate lengths. Black points are experimental values of the measured signal.

In the case of Si FETs, plasma waves in the channel are overdamped, mainly because of a relatively low electron mobility. As it was shown theoretically [7,8] in this case, a nonresonant detection signal depends exponentially on the distance (x) from the source with a parameter l_c that is a characteristic length for the plasma density distribution decay

$$U(x) = \frac{U_a^2}{4U_0}\left[1 - \exp(-2x/l_c)\right] \tag{1}$$

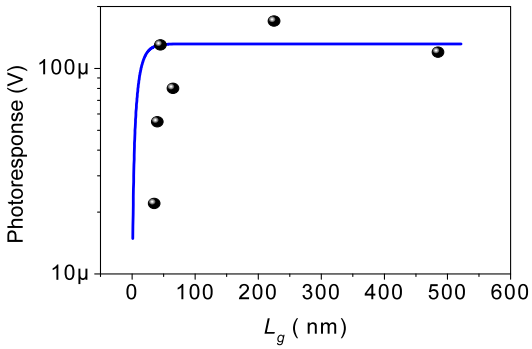

Fig. 9. Photoresponse of Si-MOSFETs versus gate length.

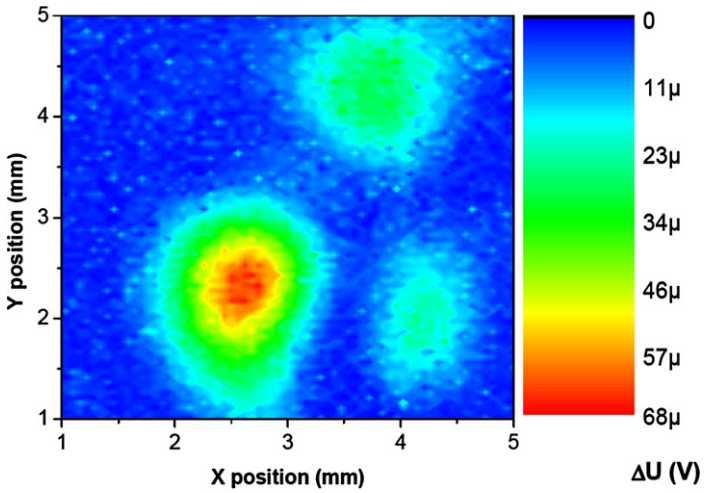

Fig. 10. Image of a nonpolarized BWO beam at 1.05 THz and at room temperature with a specially designed Silicon MOSFET detector. *X* and *Y* axes are position of the detector in mm. Right scale reflects signal in microvolts.

We assume that the channel is excited by the incident radiation at the source side. $U(x)$ is the dc voltage generated by THz rectification, U_a is the amplitude of the incident ac modulation, U_0 is the gate voltage swing. l_c characterizes the exponential decay of the plasma density perturbation away from the source. It can be written as $l_c = s(2\tau/\omega)^{1/2}$, with the plasma waves velocity $s = (eU_0/m)^{1/2}$.

In the case of short gate transistors, $L_g \ll l_c$, the ac current induced by the incident radiation goes through the gate-to-channel capacitance practically uniformly on the whole gate length, and only a part of the photoresponse dc voltage is built up. In this case, the total measured voltage is expected to depend on the gate length. On the opposite case, for long gate transistors with $L_g \gg l_c$, the ac current perurbation will leak to the gate before it reaches the drain, and the total photoresponse is built up only within a part of the channel adjacent to the source. One expects that in this case the total measured photovoltaic signal does not depend on the gate length. To avoid the signal decrease related to loading effects for long transistors the resistance of the inactive part of the channel should be much smaller than the input resistance of the measurement system. The black solid line in Fig. 9 was calculated using Eq. (1) with a fixed critical length $l_c = 100$ nm. One can see that this simple theoretical estimation gives relatively good description of the observed signal reduction.

One can often observe also a drop of the signal for long channels. This can happen especially if the preamplifier with a relatively low input resistance is used. The reason for this is that close to the threshold condition a nonactive part of the channel acts as a parasitic resistance leading to a voltage divider [19]. This effect can be very important especially at higher frequencies because the effective decay length $l_c = s(2\tau/\omega)^{1/2}$ is shorter here—it changes like the inverse of a square root of the frequency. Therefore, for detection at higher frequencies, shorter channel lengths are more suitable.

Recently, a technological improvement of the Si MOSFET based THz detectors was obtained [36]. By choosing a 130-nm technology and a proper antenna design a good responsivity at frequency above 1 THz frequency was demonstrated. The basic pixel consisted of a bow-tie antenna in the metal layers, connected to a nMOS detector. Transistors with various length and width of the channels from the minimum value allowed by the technology (130 nm) to a few micrometers were tested. The best results above 1 THz were obtained with the minimum dimensions, i.e., 130 nm in length and 250 nm in width.

The photoresponse measurements were performed using a BWO source operating at 1.05 THz with an output power of 150 µW measured by a calibrated large aperture THz power meter. In the best configuration, the detector sensitivity

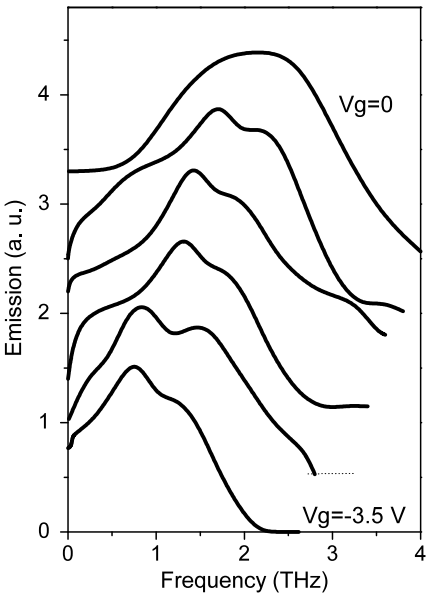

Fig. 11. Emission spectra for GaN/AlGaN transistor at $V_{ds} = 4$ V, gate biases, V_g: −3.5 V (lower curve); −3 V, −2 V, −1.5 V, −0.5 V, 0 (upper curve).

measured was equal to 50 V/W as calculated from the image surface integral normalized to the total beam power and physical pixel size. In these conditions an image of a nonpolarized BWO beam at 1.05 THz was obtained at room temperature (see Fig. 10). X and Y axes are position of the detector in mm. The signal scale shown on the right is a directly measured source–drain voltage without amplification.

5. Emission from GaN/AlGaN FETs

As already mentioned in the introduction, the interest in the applications of FETs for THz spectroscopy started at early 1990s with a pioneering theoretical work of Dyakonov and Shur [1] who predicted that a steady current flow in a FET channel can become unstable against generation of plasma waves. These waves can, in turn, lead to the emission of electromagnetic radiation at the plasma wave frequency. THz emission in nW power range from submicron InGaAs and GaN FETs has been observed both at cryogenic as well as at room temperatures [3–5]. However, in most experiments, the emission did not depend on the gate voltage as predicted in [1].

Only recently a tunable THz emission has been observed at room temperature from AlGaN/GaN-based high electron mobility transistors [15]. The samples have been grown by the MOCVD method. The gate width was 2 μm × 100 μm the gate length (L) was 250 nm. The gate of the sample was covered by the field plate. The emission signal was excited by square source–drain voltage pulses with pulse frequency 30 Hz and duty cycle 0.5, the source–gate voltage being constant. For a spectral analysis of the radiation a Fourier transform spectrometer under vacuum has been used.

The emission appeared in a threshold-like manner, and was accompanied by a drop in the drain current. Emission spectra are shown in Fig. 11. While fixing the drain bias at $V_{ds} = 4$ V, the gate bias was changed from −3.5 V to 0 V. As a consequence, one can see that the emission maxima are considerably shifted (from 0.75 to 2.1 THz). The position of the maxima of emission spectra as a function of the gate voltage is presented in Fig. 12 by points. Thus, the tunability of the emission frequency by the gate voltage is clearly shown.

The solid line in Fig. 12 presents the dependence of the fundamental frequency on the gate bias given by [1,2]

$$f = \frac{1}{4}\frac{s}{L_{eff}}\left(1 - \frac{\upsilon^2}{s^2}\right) \tag{2}$$

where $s = (eU_0/m)^{1/2}$ is the plasma wave velocity, e is the electron charge, υ is the electron drift velocity, m is the effective electron mass ($m = 0.2m_0$, where m_0 is the free electron mass) and U_0 is the gate-to-channel voltage swing. In our gate bias range the ratio υ/s is small and can be neglected. The effective gate length is the length of the channel controlled by the gate. It depends on the gate-to-channel separation d, and can be estimated as [3]: $L_{eff} = L + 2d$, where L is the geometric gate length and d is the thickness of the wide band AlGaN barrier layer. One can see that the theoretical curve fits well the experimental points.

As mentioned above, in earlier experiments [3–5] mainly a broadband, gate independent emission was observed. A possible explanation why the experimental results on THz emission from FETs in Refs. [3–5] cannot be directly compared with the theory [1] was given only recently by M. Dyakonov [8,23]. The main reason is that the transistor geometry is very different from the one-dimensional model adopted in [1]. In a standard experimental situation, the width W of the gate is much

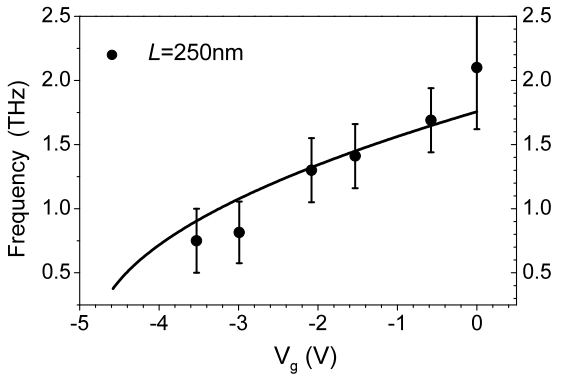

Fig. 12. Position of the emission peak as a function of gate bias for two GaN/AlGaN transistors at drain to source voltage $V_{ds} = 4$ V. Lines are calculated using Eq. (2).

larger than the gate length L. Under such conditions the one-dimensional model, where the plasma density and velocity depend on one coordinate only, is not appropriate because oblique plasma waves also can propagate. In such geometry, the gated region is not a resonator, but rather a waveguide with a continuous spectrum of plasma waves.

In Ref. [23], an analysis of the stability was extended to a more realistic case when $W \gg L$, and it was shown that in such a geometry an additional new mode of instability dominates, which is localized near the gate boundaries and results in a broad spectrum of the plasma oscillations. It is not clear up to now what are exact geometrical and electrical conditions that allow observing the tunable emission. We believe that in the case of experiments reported in this work the plasma wave excitation under the gate is favored by the presence of the field plate covering the gate on the drain side; this plate favorites boundary conditions suitable for development of plasma instability.

6. Conclusion

In conclusion, we have presented an overview of experimental results on plasma excitation in field effect transistors with nanometric gates. The excitation of plasma waves by sub-THz and THz radiation at cryogenic temperatures was demonstrated. We observed also nonresonant over-damped plasma modes in room temperature detection experiments. Recent results on voltage-tunable THz emission from GaN based FETs were discussed as well. Results on THz detection and emission allow one to propose them as new valuable elements for THz imaging and spectroscopy. Their real importance comes from the fact that using modern electronics technology many of these elements can be easily integrated to make focal plane arrays (detectors) or high power emitters (sources).

Acknowledgements

We thank M. Dyakonov for help in experiments and interpretation of the results that are reported in this review. This work was supported by CNRS, the GDR-E project “Semiconductor sources and detectors of terahertz frequencies” and by the ANR TeraGaN project. We acknowledge STMicroelectronics through the “Nano2013” project and the European Union Grant No. MTKD-CT-2005-029671. Montpellier–Vilnius cooperation is supported, in part, by Gilibert/EGIDE programme.

References

[1] M.I. Dyakonov, M.S. Shur, Shallow water analogy for a ballistic field effect transistor: New mechanism of plasma wave generation by dc current, Phys. Rev. Lett. 71 (1993) 2465.
[2] M.I. Dyakonov, M.S. Shur, Plasma wave electronics: Novel terahertz devices using two dimensional electron fluid, IEEE Trans. Electron Devices 43 (1996) 380.
[3] W. Knap, J. Łusakowski, T. Parenty, S. Bollaert, A. Cappy, V.V. Popov, M.S. Shur, Terahertz emission by plasma waves in 60 nm gate high electron mobility transistors, Appl. Phys. Lett. 84 (2004) 3523.
[4] N. Dyakonova, F. Teppe, J. Łusakowski, W. Knap, M. Levinshtein, A.P. Dmitriev, M.S. Shur, S. Bollaert, A. Cappy, Magnetic field effect on the terahertz emission from nanometer InGaAs/AlInAs high electron mobility transistors, J. Appl. Phys. 97 (2005) 4313.
[5] N. Dyakonova, A. El Fatimy, J. Łusakowski, W. Knap, M.I. Dyakonov, M.A. Poisson, E. Morvan, S. Bollaert, A. Shchepetov, Y. Roelens, Ch. Gaquiere, D. Theron, A. Cappy, Room temperature terahertz emission from nanometer field-effect transistors, Appl. Phys. Lett. 88 (2006) 141906.
[6] W. Knap, F. Teppe, N. Dyakonova, D. Coquillat, J. Łusakowski, Plasma wave oscillations in nanometer field effect transistors for terahertz detection and emission, J. Phys.: Condens. Matter 20 (2008) 384205.
[7] W. Knap, M. Dyakonov, D. Coquillat, F. Teppe, N. Dyakonova, J. Łusakowski, K. Karpierz, G. Valusis, D. Seliuta, I. Kasalynas, A. El Fatimy, T. Otsuji, Field effect transistors for terahertz detection: Physics and first imaging applications, J. Infrared Milli Terahz Waves 30 (2009) 1319.
[8] M.I. Dyakonov, Generation and detection of terahertz radiation by field effect transistors, C. R. Physique 11 (7–8) (2010) 413–420, this issue.
[9] S. Nadar, H. Videlier, D. Coquillat, F. Teppe, M. Sakowicz, N. Dyakonova, W. Knap, D. Seliuta, I. Kašalynas, G. Valušis, Room temperature imaging at 1.63 and 2.54 terahertz with field effect transistor detectors, J. Appl. Phys. (2010), in press.
[10] S. Boubanga-Tombet, M. Sakowicz, D. Coquillat, F. Teppe, N. Dyakonova, W. Knap, K. Karpierz, J. Łusakowski, Terahertz detection by field effect transistor in high magnetic fields: influence of Shubnikov–de Haas and cyclotron resonance effects, Appl. Phys. Lett. 95 (2009) 072106.

[11] M. Sakowicz, J. Lusakowski, K. Karpierz, M. Grynberg, W. Knap, K. Köhler, G. Valušis, K. Gołaszewska, E. Kaminska, A. Piotrowska, Terahertz detection by two dimensional plasma field effect transistors in quantizing magnetic fields, Appl. Phys. Lett. 92 (2008) 203509.
[12] O.A. Klimenko, Yu.A. Mityagin, H. Videlier, F. Teppe, N.V. Dyakonova, C. Consejo, S. Bollaert, V.N. Murzin, W. Knap, Terahertz response of InGaAs field effect transistors in quantizing magnetic fields, Appl. Phys. Lett. May (2010), in press.
[13] H. Videlier, S. Nadar, M. Sakowicz, T. Trinhvandam, D. Coquillat, F. Teppe, N. Dyakonova, W. Knap, T. Skotnicki, Terahertz broadband detection using silicon MOSFET, in: 16th International Conference on Electron Dynamics in Semiconductors Optoelectronics and Nanostructures (EDISON 16), 24–28 August 2009, Montpellier, France, J. Phys.: Conf. Ser. (2009), in press.
[14] R. Tauk, F. Teppe, S. Boubanga, D. Coquillat, W. Knap, Y.M. Meziani, C. Gallon, F. Boeuf, T. Skotnicki, C. Fenouillet-Beranger, D.K. Maude, S. Rumyantsev, M.S. Shur, Appl. Phys. Lett. 89 (2006) 253511.
[15] A. El Fatimy, N. Dyakonova, Y. Meziani, T. Otsuji, W. Knap, S. Vandenbrouk, K. Madjour, D. Théron, C. Gaquiere, M.A. Poisson, S. Delage, P. Pristawko, C. Skierbiszewski, AlGaN/GaN high electron mobility transistors as a voltage-tunable room temperature terahertz sources, J. Appl. Phys. 107 (2010) 024504.
[16] M. Sakowicz, J. Lusakowski, K. Karpierz, M. Grynberg, W. Knap, W. Gwarek, Polarization sensitive detection of 100 GHz radiation by high mobility field-effect transistors, J. Appl. Phys. 104 (2008) 024519.
[17] D.B. Veksler, A.V. Muraviev, T.A. Elkhatib, K.N. Salama, M.S. Shur, in: Semiconductor Device Research Symposium, 2007 International, 12–14 December 2007, p. 1.
[18] W. Knap, V. Kachorovskii, Y. Deng, S. Rumyantsev, J.-Q. Lu, R. Gaska, M.S. Shur, G. Simin, X. Hu, M. Asif Khan, C.A. Saylor, L.C. Brunel, J. Appl. Phys. 91 (2002) 9346–9353.
[19] W. Stillman, F. Guarin, V.Yu. Kachorovskii, N. Pala, S. Rumyantsev, M.S. Shur, D. Veksler, Device loading effects on nonresonant detection of terahertz radiation by silicon MOSFETs, Electron. Lett. 43 (2007) 422.
[20] W. Knap, Y. Deng, S. Rumyantsev, M.S. Shur, Resonant detection of subterahertz and terahertz radiation by plasma waves in submicron field-effect transistors, Appl. Phys. Lett. 81 (2002) 4637.
[21] W. Knap, Y. Deng, S. Rumyantsev, J.-Q. Lu, M.S. Shur, C.A. Saylor, L.C. Brunel, Resonant detection of subterahertz radiation by plasma waves in a submicron field-effect transistor, Appl. Phys. Lett. 80 (2002) 3434.
[22] A. El Fatimy, F. Teppe, N. Dyakonova, W. Knap, D. Seliuta, G. Valušis, A. Shchepetov, Y. Roelens, S. Bollaert, A. Cappy, S. Rumyantsev, Resonant and voltage-tunable terahertz detection in InGaAs/InP nanometer transistors, Appl. Phys. Lett. 89 (2006) 131926.
[23] M.I. Dyakonov, Boundary instability of a two-dimensional electron fluid, Semiconductors 42 (2008) 984.
[24] V.V. Popov, O.V. Polischuk, W. Knap, A. El Fatimy, Broadening of the plasmon resonance due to plasmon–plasmon intermode scattering in terahertz high-electron-mobility transistors, Appl. Phys. Lett. 93 (2008) 263503.
[25] V. Ryzhii, A. Satou, W. Knap, M.S. Shur, Plasma oscillations in high-electron-mobility transistors with recessed gate, J. Appl. Phys. 99 (2006) 084507.
[26] I. Khmyrova, Yu. Seijyou, Analysis of plasma oscillations in high-electron mobility transistor-like structures: Distributed circuit approach, Appl. Phys. Lett. 91 (2007) 143515.
[27] A. Shchepetov, C. Gardès, Y. Roelens, A. Cappy, S. Bollaert, S. Boubanga-Tombet, F. Teppe, D. Coquillat, S. Nadar, N. Dyakonova, H. Videlier, W. Knap, D. Seliuta, R. Vadoklis, G. Valušis, Oblique modes effect on terahertz plasma wave resonant detection in InGaAs/InAlAs multichannel transistors, Appl. Phys. Lett. 92 (2008) 242105.
[28] S. Boubanga-Tombet, F. Teppe, D. Coquillat, S. Nadar, N. Dyakonova, H. Videlier, W. Knap, A. Shchepetov, C. Gardès, Y. Roelens, A. Cappy, S. Bollaert, D. Seliuta, R. Vadoklis, G. Valušis, Current driven resonant plasma wave detection of terahertz radiation: Toward the Dyakonov–Shur instability, Appl. Phys. Lett. 92 (2008) 212101.
[29] T. Otsuji, M. Hanabe, T. Nishimura, E. Sano, A grating-bicoupled plasma-wave photomixer with resonant-cavity enhanced structure, Opt. Express 14 (2006) 4815;
T. Otsuji, Y.M. Meziani, M. Hanabe, T. Ishibashi, T. Uno, E. Sano, Grating-bicoupled plasmon-resonant terahertz emitter fabricated with GaAs-based heterostructure material systems, Appl. Phys. Lett. 89 (2006) 263502.
[30] D. Coquillat, S. Nadar, F. Teppe, N. Dyakonova, S. Boubanga-Tombet, W. Knap, T. Nishimura, T. Otsuji, Y.M. Meziani, G.M. Tsymbalov, V.V. Popov, Room temperature detection of sub-terahertz radiation in double-grating-gate transistors, Opt. Express 18 (2010) 6024.
[31] W. Knap, F. Teppe, Y. Meziani, N. Dyakonova, J. Lusakowski, F. Boeuf, T. Skotnicki, D. Maude, S. Rumyantsev, M.S. Shur, Appl. Phys. Lett. 85 (2004) 675.
[32] A. Lisauskas, W. von Spiegel, S. Boubanga, A. El Fatimy, D. Coquillat, F. Teppe, N. Dyakonova, W. Knap, H.G. Roskos, Terahertz imaging with GaAs field-effect transistors, Electron. Lett. 44 (2008) 408.
[33] A. Lisauskas, U. Pfeiffer, E. Öjefors, P.H. Bolìvar, D. Glaab, H.G. Roskos, Rational design of high-responsivity detectors of terahertz radiation based on distributed self-mixing in silicon field-effect transistors, J. Appl. Phys. 105 (2009) 114511.
[34] A. El Fatimy, J.C. Delagnes, E. Abraham, E. Nguema, P. Mounaix, F. Teppe, W. Knap, Plasma wave field effect transistor as a resonant detector for 1 terahertz imaging applications, Optics Commun. 282 (2009) 3055.
[35] M. Lifshits, M. Dyakonov, Photovoltaic effect in a gated two-dimensional electron gas in magnetic field, Phys. Rev. B 80 (2009) 121304.
[36] F. Schuster, H. Videlier, D. Coquillat, M. Sakowicz, F. Teppe, B. Dupont, B. Giffard, W. Knap, Imaging above 1 THz limit with Si-MOSFET detectors, in: IRMWW Conference Rome, 2010, in press.